Global Prospects for Utility-Scale Solar Power: Toward Spatially Explicit Modeling of Renewable Energy Systems

Kevin Ummel

Abstract

This paper provides high-resolution estimates of the global potential and cost of utility-scale photovoltaic and concentrating solar power technologies and uses a spatially explicit model to identify deployment patterns that minimize the cost of greenhouse gas abatement. A global simulation is run with the goal of providing 2,000 TWh of solar power (~7% of total consumption) in 2030, taking into account least-cost siting of facilities and transmission lines and the effect of diurnal variation on project profitability and required subsidies. The American southwest, Tibetan Plateau, Sahel, and Middle East are identified as major supply areas. Solar power consumption concentrates in the United States over the next decade, diversifying to Europe and India by the early 2020's, and focusing in China in the second half of the decade—often relying upon long-distance, high-voltage transmission lines. Cost estimates suggest deployment on this scale is likely to be competitive with other prominent abatement options in the energy sector. Further development of spatially explicit energy models could help guide infrastructure planning and financing strategies both nationally and globally, elucidating a range of important questions related to renewable energy policy.

Keywords: photovoltaic, concentrating solar, solar thermal, mitigation, carbon abatement, energy economics, electricity transmission, climate change

Center for Global Development
www.cgdev.org

Working Paper 235
December 2010

Global Prospects for Utility-Scale Solar Power: Toward Spatially Explicit Modeling of Renewable Energy Systems

Kevin Ummel
Senior Visiting Associate
Center for Global Development

MESPOM Candidate
University of Manchester

Contact address: publications@cgdev.org

Many thanks to Nancy Birdsall, Ray George, Donna Heimiller, Robert Hijmans, Thomas Huld, Robin Kraft, Jan Lundquist, Lawrence MacDonald, Amy Milam, Anthony Patt, Liliana Rojas-Suarez, David Roodman, Jacob van Etten, Dirk Westermann, and David Wheeler for technical assistance, data, and comments. All remaining errors are the author's alone.

CGD is grateful for contributions from the Australian Agency for International Development in support of this work.

Kevin Ummel. 2010. "Global Prospects for Utility-Scale Solar Power: Toward Spatially Explicit Modeling of Renewable Energy Systems." CGD Working Paper 235. Washington, D.C.: Center for Global Development.
http://www.cgdev.org/content/publications/detail/1424669

Center for Global Development
1800 Massachusetts Ave., NW
Washington, DC 20036

202.416.4000
(f) 202.416.4050

www.cgdev.org

Foreword

The power sector accounts for about 29 percent of global greenhouse gas emissions. In this sector, mitigation requires switching from fossil fuels to low-carbon energy sources, principally solar, wind, biomass, geothermal, hydro, and nuclear. The conventional narrative assigns the task of developing clean energy to rich countries because it is perceived to be too costly for poor countries. The reality, however, is far different: since 1990, developing countries have accounted for 55 percent of the global increase in low-carbon energy generation. Since 2000, China and India have exceeded the United States and matched other rich countries in their share of national income devoted to subsidizing low-carbon energy (Wheeler 2010). And both China and India have announced ambitious plans for renewable energy development during the coming decade (Wheeler and Shome 2010). The implication is clear: clean energy development will be a truly global undertaking.

In this path-breaking paper, Kevin Ummel shows how the global undertaking can unfold for solar power. Kevin's work builds on his two previous papers. The first supported the Clean Technology Fund's pioneering investment in North African concentrating solar power (CSP) (Ummel and Wheeler 2008). The second (Ummel 2010) demonstrated that India and China have enormous solar potential, identified their feasible generation sites, and analyzed the cost of a CSP development program that could deliver 20 percent of their total power generation by 2050. Under reasonable assumptions about learning and scale economies, this program could make CSP cost-competitive with coal-fired power within two decades.

Kevin's new paper extends his work to the global arena, and broadens it to include photovoltaic (PV) power as well as CSP. He estimates the power potential and cost of utility-scale PV and CSP and develops a global deployment scenario that would minimize the cost of greenhouse gas abatement by exploiting learning economies and local differences in solar economics. His scenario would deliver about 2,000 TWh of solar power (about 7 percent of global power consumption) in 2030. Kevin's analysis is summarized by

global maps in Figures 1 and 7 of the paper. Figure 1 displays potential utility-scale solar power sites worldwide, along with estimated, fully-accounted costs of power delivered from those sites. The broad geographic variation of estimated costs in Figure 1 provides striking support for Kevin's proposed global rollout plan, which would start by exploiting learning and scale economies at the least costly sites. Figure 7 translates Kevin's scenario into a map of first-phase solar production and transmission systems that could be operational by 2030 in Asia, Africa, Latin America, North America, Europe, and Australia.

Kevin's main message in the paper is simultaneously visionary and practical: massive global deployment of solar power is within reach, if we have the collective will to promote it, and affordable, if we adopt a sensible deployment strategy. Let us hope that we have the collective will and intelligence to pursue this vision successfully. The implications are particularly critical for poor countries, which are already hard-hit by climate changes that they are ill-equipped to confront.

David Wheeler
Senior Fellow
Center for Global Development

I. INTRODUCTION

Volatile fuel prices, supply disruptions, local air pollution, and global climate change threaten life and welfare, particularly in developing countries. A shift toward renewable, clean sources of energy would help mitigate such risks. Electricity generation currently relies upon fossil fuels for ~70% of output and is responsible for nearly 30% of all greenhouse gas (GHG) emissions (IPCC 2007; IEA 2009). The sector is a good candidate for rapid and widespread transformation, because renewable power technologies (especially wind and solar) are well-developed and commercially available, and electricity is a versatile energy carrier capable of displacing fossil fuel in other sectors. But renewable power deployment faces different challenges than fossil-fuel-based systems. While humans largely dictate the location and timing of electricity generation at present, a renewable future will emphasize intelligent *harvesting* of energy that – while free, clean, and plentiful – may also be spatially diffuse and temporally irregular.

Factors that are effectively controlled in present power systems (like generating efficiency and output) vary significantly over space and time in renewable systems. Operation is possible only in certain locales, and profitability is closely linked to the quantity, quality, and timing of the resource (wind, sunlight, tides, etc.). It may also be necessary to transmit power from remote generating sites to consumption centers, introducing a suite of additional constraints. In this context, intelligent planning – by either the private or public sector – must consider a wide range of socioeconomic, technical, and geophysical information. Making the best use of renewable resources requires that this "spatiotemporal" complexity be explicitly incorporated into modeling and analysis of alternative energy futures. The financing and infrastructure decisions critical to the future of renewable energy should be informed by modeling of multiple technologies across large areas over many years – and at relatively high spatiotemporal resolution – in order to capture the complex interactions of energy economics, resource availability, and engineering requirements.

Toward that end, this paper provides high-resolution estimates of potential output for three large-scale solar power technologies. These estimates are then incorporated into a simple, spatially-explicit deployment model to identify least-cost siting of generating facilities and high-voltage transmission lines at global scale, taking into account a number of important factors affecting the profitability of solar power projects. The objective is to minimize the cost of averting greenhouse gas emissions from coal power plants, which are projected to rise by ~50% over the next 20 years (IEA 2009). The results are spatial in nature, revealing the particular sites and line routes that make optimal use of available sunlight. Combined with information on construction costs, financing, and power prices, it is possible to estimate the public subsidies required for large-scale deployment.

The analysis is limited to three utility-scale solar technologies: photovoltaic (PV), concentrating solar power (CSP), and CSP with thermal storage. This study does *not* include "rooftop" photovoltaics; references to "solar power" refer to large-scale installations only.[1] Many of the concepts and model assumptions, however, are applicable to a range of renewable power sources – including rooftop PV, wind, biomass, and geothermal – or even non-renewable technologies like carbon capture and storage (CCS) that are also spatially-defined. Section VII explores the potential for spatially-explicit modeling of energy systems to elucidate a range of important questions.

Section II describes how candidate solar power sites are identified and potential performance and cost determined. Section III reports worldwide techno-economic potential based on high-resolution analysis of terrain and meteorological factors. Section IV outlines transmission engineering requirements and cost assumptions. Section V describes the basic modeling approach and data requirements. Section VI reports the result of illustrative model run in which solar power attempts to provide 2,000 TWh of electricity worldwide in 2030.

II. PLANT SITING, PERFORMANCE, AND COST

The technologies assessed include semi-crystalline silicon photovoltaic arrays (PV), concentrating parabolic trough (CSP) and parabolic trough with six hours of molten salt thermal storage (CSPTS). Unlike PV technology, CSP uses mirrors to concentrate sunlight and produce steam that can be used in a conventional generator set. Thermal storage allows excess heat generated during the day to be stored and utilized later. It must be noted that thermal storage remains largely untested in commercial settings and the assumptions here are somewhat speculative. Further, there is no consideration of hybrid gas-CSP systems, which may prove quite useful (Zhang et al. 2010). Output from PV arrays cannot be stored and must be used at the time of generation.[2]

Installations are best placed on flat, open terrain free from obstructions, settlements, or dangerous land features. Following the methodology of Ummel (2010), the GlobCover land cover database (~300 m resolution) is used to identify suitable areas in conjunction with data on slope, population density, and geomorphology at ~1 km resolution (Verdin et al. 2007; Bicheron et al. 2008; ORNL 2008; FAO et al. 2009). Additionally, protected areas are excluded, safety buffers applied to screened areas, and a consolidation algorithm used to retain only contiguous tracts of at least 3 km^2 (IUCN and UNEP 2010).[3]

[1] Future solar power generation could be spatially *distributed* among consumers (via rooftop photovoltaic power, for example) or *centralized* in strategic locales from which electricity is transmitted to demand centers. This paper addresses only the latter mode. Consequently, an important and contested question – Which mode of generation should we pursue? – is not addressed.

[2] The PV arrays are set on open racks at latitudinal tilt; all technologies employ single-axis tracking. Both CSP configurations use evaporative cooling; see Section VII for more on water consumption.

[3] Facilities are restricted to bare areas, sparse vegetation, or shrubland. Additional screens eliminate cells with average slope >3%, population density >150 people per km^2, or evidence of flooding, artificial surfaces, permanent ice or snow, glaciers, sand dunes, salt flats, or rock outcrops. Safety buffers range from 1 km for coastlines and artificial surfaces to 6 km for sand dunes.

The quantity and type of solar radiation are key determinants of overall plant performance. PV technology can utilize all radiation falling on the cell: both the direct sunlight component and diffuse radiation scattered by clouds and aerosols (together, *global horizontal irradiance* or GHI*)*. CSP utilizes only the direct beam perpendicular to the receiver (*direct normal irradiance* or DNI*)*. Monthly average GHI and DNI at a resolution of ~40 km are provided by the U.S. National Renewable Energy Laboratory (NREL) for most of Latin America, Africa, and East Asia. Higher resolution (~10 km) data are available for the U.S., Afghanistan, and Pakistan (NREL 2005). For areas not covered by these datasets, NASA's global SSE product (~100 km resolution) is used (NASA 2009).[4]

Local weather conditions, especially ambient temperature, have a secondary effect on performance. In the case of PV panels, for example, efficiency falls with increasing temperatures. Hourly data on relevant radiation and weather variables are available for only a limited number of sites worldwide, typically in urban areas unsuited for utility-scale installations. High-quality data are available for U.S. sites, however, through NREL's Solar Prospector. A clustering algorithm is used to select U.S. sites thought to be representative of suitable areas worldwide on the basis of average annual radiation and temperature. Solar plant performance at the representative sites is modeled with NREL's Solar Advisor Model (SAM), which provides detailed, hourly modeling of plant performance given local weather conditions (Gilman et al. 2008). Cost-minimizing plant configuration is determined for each technology and linear regressions fit to the results to predict monthly plant capacity factor as a function of average monthly radiation (GHI or DNI) and temperature.[5] These are used to predict annual capacity factors for each technology and candidate cell at ~10km resolution.[6]

Predicted capacity factors are combined with capital and operating cost (Table 1) and financing assumptions (Table 2) to estimate the levelized cost of electricity (LCOE) for each technology and candidate cell. This is the LCOE "at the gate" – that is, before the additional cost of transmission – and so describes the minimum average revenue required for financial sustainability.

[4] A global, consistent, high-resolution (<=10 km spatial and ~1-hour temporal) solar radiation dataset would be ideal. Such data are derived from satellite measurements by a small number of commercial providers; the data are costly and generally used for single-site analysis. Since radiation values can change significantly in response to local conditions and time, and utility-scale (~250 MW) installations can cover less than 10 km^2, using average radiation values across grid cells of up to ~10,000 km^2 is obviously a gross simplification. The highest-resolution, publically-available data have been used here, but model uncertainty could be reduced by investing in higher-resolution data.

[5] Capacity factors are modeled as $C \equiv \alpha + \beta R + \delta RT$, where C is the monthly capacity factor, R is the monthly radiation (GHI for PV, DNI for CSP), and T is the monthly average temperature. Coefficients β and δ are highly significant in all cases and R^2 is ~0.90; this form allows for a partial effect of temperature. For prediction, satellite-derived radiation and monthly, spatially-interpolated temperature data are used as RHS inputs (Hijmans et al. 2005).

[6] The lack of high-quality meteorological data for a diverse set of locales restricts the confidence in capacity factor prediction. For example, the U.S. data from which representative sites are drawn contains no sites with exceptionally high GHI and temperature like those observed in suitable locales in Africa and Australia, nor sites with exceptionally high DNI but low temperature as seen on the Tibetan Plateau. As a result, prediction necessarily occurs outside the range of the input data for many sites of interest worldwide. More data (especially hourly data) are needed to better specify plant performance under "extreme" conditions.

Table 1: Solar power plant cost and operating assumptions

	Capital Cost ($ per kW)	Annual O&M ($ per kW)	Land use (MW per km^2)	Life cycle emissions (gCO_2eq per kWh)
Photovoltaic (PV)	5,000	50	35	90
Parabolic trough (CSP) no thermal storage	4,000	80	31	30
Parabolic trough (CSPTS) 6-hour thermal storage	7,000	140	23	40

Table 2: Solar power plant financing assumptions

Project lifetime	Debt/equity ratio	Loan interest rate	Required return on equity	Capital recovery factor
30 years	40/60	8%	15%	12.6%

For CSP configurations, minimizing the cost of production requires optimizing the size of the mirror array ("solar multiple"). For CSP without storage, the optimal solar multiple is ~1.4 for representative sites; with storage it ranges from 2.1 to 2.5 depending on the locale.[7] In the case of thermal storage, true maximization of *profits* depends on daily and seasonal variation in the price of electricity since plant operators can somewhat control the timing of sales to the grid. This consideration is roughly incorporated in the SAM simulations via a dispatch schedule that prioritizes output during peak-price afternoon periods. The consequences of diurnal price variation are covered in more detail in Section V.

III. GLOBAL DISTRIBUTION OF SOLAR POTENTIAL AND COST

Figure 1 shows the extent of areas suitable for utility-scale solar installations and the estimated cost of production in those locales, given the cost assumptions in Tables 1 and 2. The reported LCOE is the minimum for each cell of the three solar technologies assessed. This is the cost of production "at the gate" and does not account for the cost of transmitting electricity to demand centers or differences in timing or magnitude of electricity prices, which can affect both overall profitability and choice of technology (those factors are addressed in Sections IV and V). It also ignores other factors, like accessibility and local material and labor costs, which could significantly impact actual projects. Given the cost assumptions noted above, however, Figure 1 does show the relative distribution of production costs in response to varying radiation levels and temperature.

[7] A solar multiple of one describes a mirror array capable of supplying the generator with sufficient steam at maximum capacity, assuming maximum annual DNI incident on the receivers. Solar multiples above one will generate excess heat during peak DNI periods (stored in TS configurations and "dumped" otherwise), but the extra generation at non-peak times may offset the cost of additional mirrors.

Figure 1: Potential utility-scale solar power sites and predicted ("at the gate") LCOE

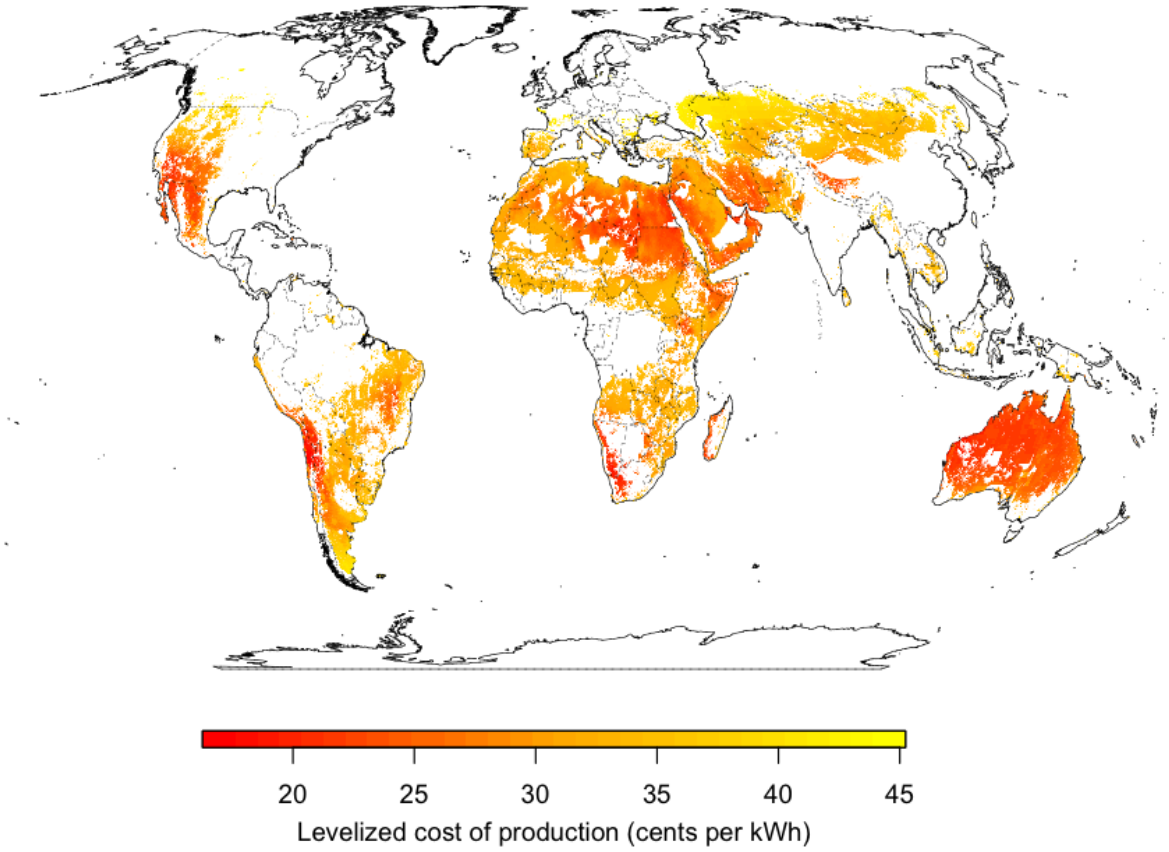

Globally, the potential of utility-scale installations exceeds 1,500 petawatt-hours (PWh) per year. Australia alone, with its massive expanses of uninhabited, sunny outback, contains 20% of the total. Even when restricted to areas with estimated cost below 30 cents per kWh, global technical potential exceeds 800 PWh annually. At present, total global power consumption is less than 20 PWh per year (IEA 2009). Figure 2 shows low-cost potential in major electricity-consuming economies, relative to current consumption. Since this pertains only to utility-scale installations, countries may show zero potential despite promoting PV for buildings.

Figure 2: Potential utility-scale solar power output (<30 cents per kWh) relative to current consumption

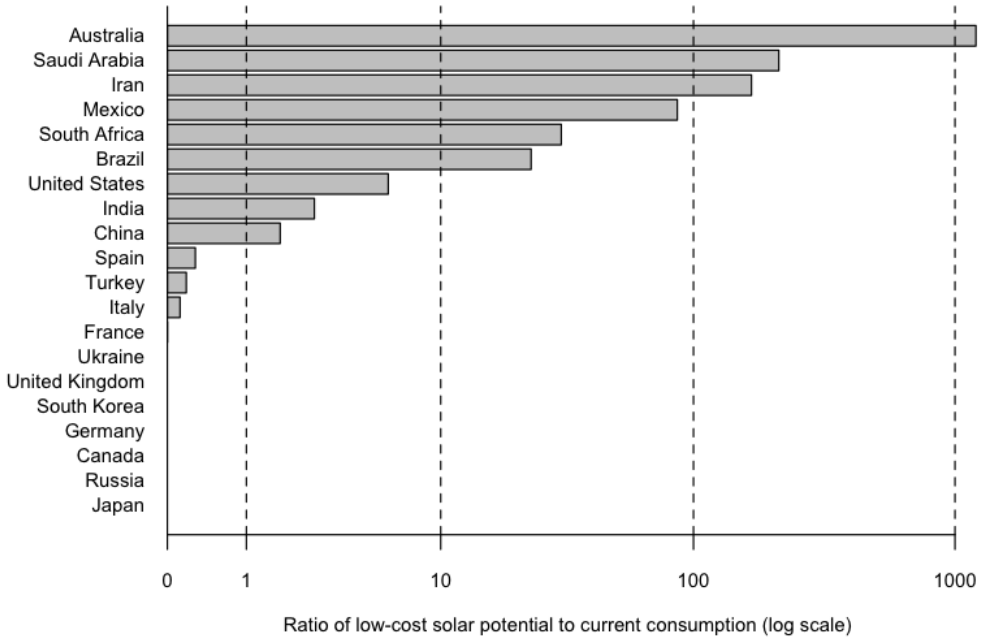

The cost distribution of potential differs significantly between countries. In some places, potential is concentrated in areas with high-quality solar resources where the cost of production is expected to be quite low; in others, overall potential may be high but spread across large expanses with only low-to-moderate radiation levels. Figure 3 shows the amount of utility-scale solar power production in each country at or below a given cost point – akin to a rough supply curve. Australia and South Africa, for example, have extensive potential below 20 cents per kWh. Spain and India, on the other hand, face higher initial costs that escalate as output increases and production is forced to utilize marginal locales.

Estimates of technical potential and the cost of production reveal little about barriers (economic or physical) to moving electricity from production sites to consumption centers. Figure 1 suggests that there is generally low correlation of optimal generating sites and the location of electricity consumption – as should be expected if dry, flat, and often hot places provide the best solar resource. Utility-scale solar power will need to utilize extensive transmission infrastructure to supply consumption centers in eastern China, southern India, the eastern U.S., and Europe.

Figure 3: Potential cost of production and cumulative output in select countries

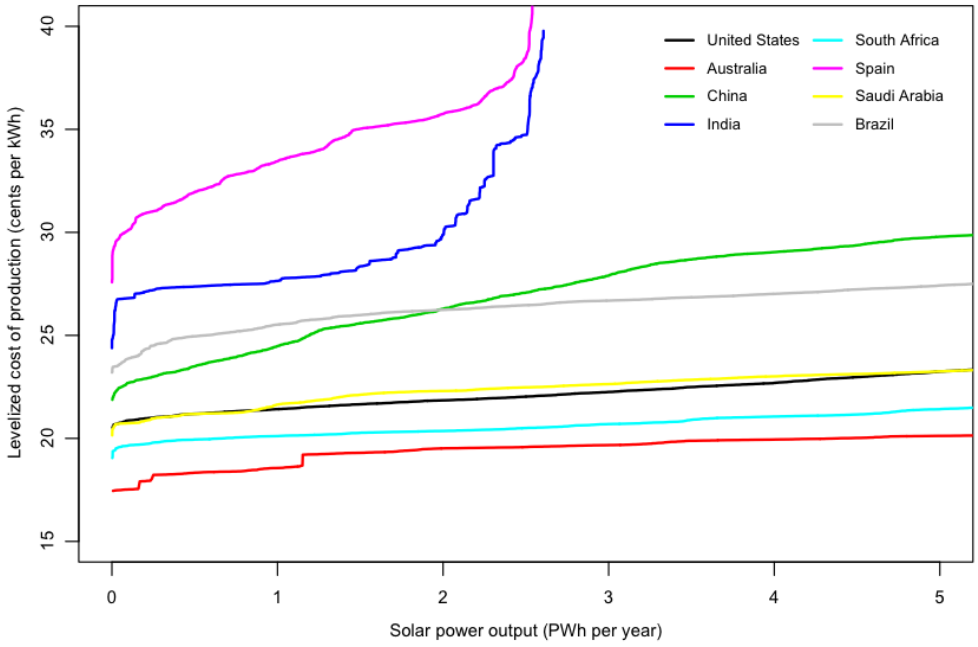

IV. TRANSMISSION REQUIREMENTS AND COST

In the absence of extensive electric grids with excess capacity, solar power must be transmitted from a substation near the site of generation to a substation connected to the desired distribution grid. Electricity grids are extremely complex; the objective here is not to model grids *per se* but to specify potential long-distance, dedicated transmission infrastructure designed to connect solar power installations to primary consumption areas. Since the issue of transmission cost is critical to the feasibility of utility-scale solar power, it is treated separately and in more detail in this section. Section V will describe the basic deployment model, which uses the assumptions outlined here to "build" transmission infrastructure where it is needed.

For linkages of the length and capacity envisioned for large-scale renewable power, a choice must be made between high-voltage alternating current (HVAC) and high-voltage direct current (HVDC) transmission technology. HVAC is the conventional choice and economically preferable for distances up to 800 to 1,200 km, beyond which the lower line costs and resistive losses of HVDC outweigh the higher fixed cost of converter stations. Overhead lines are cheapest, though it is possible to bury cables when traversing sensitive areas or making water crossings. There is an inherent tradeoff between cost and line losses, which must be optimized for each linkage individually.

The cost of transmission is difficult to specify, because details for large projects are rarely made public. Labor can constitute about 45% of the total cost of a transmission line, which is likely to be cheaper in developing countries. On the other hand, expensive conductors and converter station technology are supplied by a limited number of companies in the developed world. The following cost structure is used globally for "baseline" transmission infrastructure, assuming lowest-cost terrain and conditions. It is

based on HVDC data from CIGRE (2009) and input from industry representatives. HVAC transmission is assumed to ~140% and 35% of HVDC line and station costs, respectively.

Table 3: Transmission reference cost assumptions (lowest-cost terrain; +/- 500 kV configuration) [8]

	HVAC	HVDC	Units
Overhead lines	$815	$570	$ thousand per km
Converter stations (2)	$70	$200	$ per kW rated power

Line and station costs are allowed to vary with system power and voltage, following relationships identified by CIGRE (2009). Lines capable of higher voltages cost significantly more; moving from the reference +/- 500 kV configuration to +/- 800 kV, for example, can increase per km line costs by ~75%. Depending on the power rating and length of a connection, increasing the voltage may improve overall profitability by reducing transmission losses. The overall cost of delivered electricity is minimized within the model, taking into account the cost of infrastructure and resistive losses in the line itself. The algorithm selects from distinct line configurations at presently available voltages of +/- 300, +/-500, +/- 600, and +/- 800 kV. In general, the cost of transmission will decline with rated power as long as line voltage can also increase. If voltage is capped at +/- 800 kV (the present commercial maximum for HVDC), then costs cease to fall at loads beyond about 6,000 MW. In order to include the possibility of future transmission at power ratings up to 10,000 MW, a hypothetical +/- 900 kV line configuration is allowed in model years after 2015.

Figure 4 shows how transmission line length and power rating impact the cost profile of a hypothetical CSP plant. It only makes sense to build long transmission lines when a large amount of power is to be transmitted. For example, connecting a CSP installation with a maximum capacity of 1,000 MW to a load center 3,000 km away will result in a levelized cost of delivered electricity ~50% higher than the "at the gate" cost of generation. If the generating site is able to provide 10,000 MW, however, the overall cost increase is only ~20%. The curve for 10,000 MW assumes +/- 900 kV line voltage; higher future voltages would likely reduce the cost of long-distance, bulk power transmission even further.

[8] In the case of HVDC, assumes +/- 500 kV bipolar line with three conductors, MCM = 1,590, and rated power = 2,000 MW. A capital recovery factor of 10.6% and annual operation and maintenance equal to 2% of capital costs is assumed for calculation of levelized costs within the model.

Figure 4: Illustrative cost of transmission for CSP plant (capacity factor = 0.30)

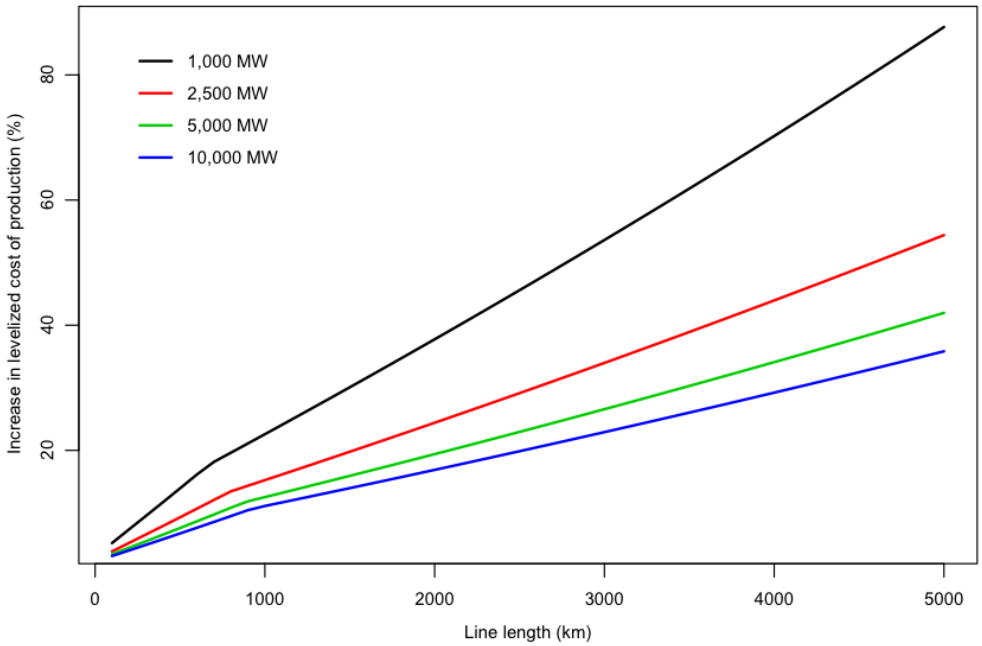

The reference cost structure applies to construction over open, unobstructed land. The model provides spatially-explicit selection of line routes, dependent upon terrain and geomorphology. Lines are excluded from steep terrain with average slope above 30%, sea floor depths greater than 2,000 meters below the surface, as well as glaciers, sand dunes, salt flats, and rock outcrops. When crossing terrain with different land covers (or underwater), the cost factors in Table 4 are applied to reference line costs. The values are very roughly informed by terrain preferences and submarine cable specifications in EPRI (2006) and Van Eeckhout et al. (2010), respectively.

Table 4: Transmission line cost markup by terrain class

	Bare or sparse vegetation	Forests	Cropland	Rice paddies	Wetlands or mangroves	Sub-marine	Urban areas or permanent snow
Cost factor	1.0	1.1	1.2	1.3	1.4	1.4	1.5

The overall cost of transmission is a function of the cost of the line and converter stations (taking into account land cover), line length (calculated as the topographic distance using average slope in each cell along the path), and the amount of power to be moved through the line (accounting for resistive losses).

V. MODELING APPROACH AND ASSUMPTIONS

Few attempts have been made to model the spatially-explicit deployment of renewable power at continental or global scales. Czisch (2006) and Aboumahboub et al. (2010) are the only studies (to the author's knowledge) similar in spirit to this one; the former focused on Europe and North Africa, the

latter being global. Both studies, however, operate at relatively coarse spatial resolution, do not account for geographical or technical barriers to transmission, and are designed to explore 100% renewable penetration rather than the cost of GHG abatement at moderate (and, most likely, realistic) levels of deployment. They do, however, incorporate multiple generation technologies, allowing them to assess the relative merits of competing technologies. In the U.S., extensive studies prepared by and for the Department of Energy have analyzed transmission requirements for wind and solar power integration (DOE 2008; EnerNex 2010; GE Energy 2010). The Regional Energy Deployment Model (ReEDS) developed by NREL is notable for its ability to assess multiple technologies and account for a number of grid operation requirements, but it relies on electricity grid data that are not readily available for global analyses (Sullivan et al. 2009).

Ultimately, there are unavoidable tradeoffs that must be made in any modeling effort. The model introduced here is an attempt to maximize the spatiotemporal coverage and resolution subject to computing and data constraints inherent to large-scale analysis. The overall goal is to identify the optimal spatiotemporal pattern of deployment, assuming that a specified deployment schedule (a quota expressed in solar power output per year) is to be met over time and that it is to be done in a manner that minimizes the cost of averting GHG emissions from coal power plants. The model is not a linear-programming model common to smaller-scale power system modeling, but a comparatively simple "step-by-step" algorithm. The code is written in the "R" language and borrows heavily from the "raster" and "gdistance" packages for manipulation of gridded spatial data and least cost path analysis, respectively (Hijmans and Van Etten 2010; Van Etten 2010).

Conceptually, production and consumption of power occur in unique "zones". Each zone contains a single "node" from (or to) which transmission may occur. The nodal points are, in turn, assigned aggregate information for all of the cells within a zone (i.e. average price of production, total consumption, etc.). Transmission occurs between pairs of nodes ("dyads"). At each point in time, the cost of GHG abatement is calculated for all dyads. An allocation algorithm begins with the lowest-cost dyad, deploys the maximum amount of solar power given the dyad's particular characteristics, and proceeds to increasingly costly dyads until all production or consumption is exhausted or (more likely) the specified deployment schedule has been fulfilled.

Zones and nodal points are identified within the model via spatial neighborhood analysis of consumption and potential solar power output. Ideally, the consumption zones would trace the outline of physical grids or balancing areas, but the data required to do this is not readily available. Instead, an algorithm attempts to identify areas where consumption or production are concentrated and create zones of a specified diameter around them (400 km for consumption; 200 km for production)**.** In order to reduce computation time, only the most promising zones – those with large amounts of coal power (consumption) or low cost solar power (production) – are retained for modeling runs. In the global scenario described in Section VI, ~170 consumption and ~600 production zones are used.

Solar power is assumed to *only* displace the construction of *new* coal power plants. The amount of new coal builds in any zone-period is the sum of new builds resulting from growth in consumption and those resulting from replacement of retired coal capacity. Following the technique applied to China and India by Ummel (2010), national estimates of electricity consumption are combined with high-resolution data

on stable nighttime lights to estimate the spatial distribution of power consumption at ~10 km resolution (NOAA 2009). IEA regional electricity consumption projections through 2030 are used estimate future cell consumption for each model period (IEA 2009). The Platts World Electric Power Plant Database is used to estimate the rate of coal plant retirements over time for each country, based on the vintage of existing capacity. The Carbon Monitoring for Action (CARMA) database is used to estimate the spatial distribution of existing coal generation (Wheeler and Ummel 2008). More than 70% of total electricity generation and 80% of coal power generation is approximately geolocated in CARMA. Coal generation not geolocated is assumed to be allocated in proportion to total consumption. It is assumed that *new* consumption over time is to be met using the present fuel mix.

The potential solar contribution in a given consumption zone is also limited by practical constraints within the grid. This is due to the fact that some non-solar generating capacity will remain minimally active – even during periods of maximum solar power generation – since the cost of shutdown and restart is prohibitive. A minimum system "turndown rate" of 30% is assumed, meaning that non-solar generation must be at least 30% of peak generation at any one moment (Denholm and Margolis 2006). This implies a maximum theoretical solar contribution of 70% of total consumption, though in practice penetration is much lower as a result of imperfect matching between the timing of supply and demand (see Figure 5 below).

The cost of GHG abatement ($ per tCO_2eq) is the cost *to the public* of averting GHG emissions from a reference (or "counterfactual") generation technology used in the absence of solar power – in this case coal power:

$$Cost\ of\ abatement\ = \frac{Solar\ LCOE\ (including\ transmission)\ -\ Average\ revenue}{Coal\ power\ emissions\ intensity\ -\ Solar\ power\ emissions\ intensity}$$

Note that steam coal prices are *not* explicitly considered when calculating the abatement cost. In theory, rising fossil fuel prices would impact the average revenue in the numerator by driving up the price of electricity. For the sake of simplicity, however, electricity prices are assumed to remain constant (see below), effectively eliminating coal price projections from the analysis.

Together, Sections III and IV describe how the cost of providing solar power from a given production site is estimated. The additional cost of transmission must be determined "on-the-fly" within the model, since the maximum power for a given dyad (which determines engineering requirements, cost, and losses) can change over time as other dyads appropriate consumption or production from a shared node. An implementation of Dijkstra's least-cost path algorithm is used to identify the cost-minimizing transmission line route for each dyad (Dijkstra 1959; Van Etten 2010). The input datasets used to determine path routing are available at ~1-2 km resolution. For global analysis, however, a degraded cost surface at ~25 km resolution is used to reduce computation time.

This study makes an important departure from many previous analyses of solar power economics by focusing not on the comparative *cost* but the comparative *profitability* of projects. While it is common to compare the cost of production between alternative generating technologies, such a comparison only yields a clear preference when revenue per kWh is equal across technologies. In the case of solar power,

which often generates electricity at moments of higher demand and, hence, higher prices, the average revenue per kWh may be significantly higher than that of conventional technologies that produce continuously.

Revenue to the solar generator is assumed to depend on the reported, annual average price of electricity at the site of consumption and the degree of temporal alignment between production and consumption. Figure 5 illustrates this concept using hourly output curves estimated from simulation of solar power plants for representative locales and hourly load and price curves based on averaged annual data from electricity markets in North America, Europe, and Australia (Li and Flynn 2004).

Figure 5: Assumed diurnal trends for price, load, and solar power output

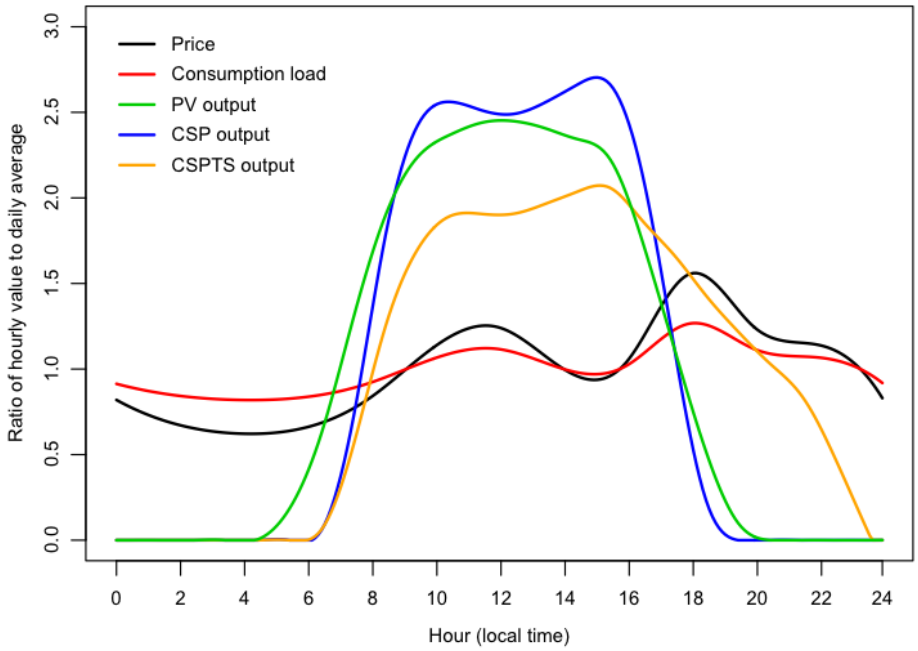

Given these diurnal patterns, the daytime output of solar technologies results in average revenue per kWh 8-15% higher than a generating technology with uniform (constant) output. CSP with 6-hour thermal storage is able to further "push" output into the peak evening price period. If production and consumption occur in the same time zone, this will result in average revenue per kWh ~5% higher than PV or CSP without storage. For all technologies, production located to the west of consumption will shift the output curves to the right in Figure 5 (assuming the horizontal axis refers to local time at the point of consumption). Consequently, the east-west orientation of sites impacts average revenue and is accounted for in the model via a simple time shift of one hour for every 15 degrees of longitude. Notice that east-west orientation is potentially important in cases of long-distance (continental-scale) transmission, especially when generating potential is concentrated to the west of demand centers. This happens to be a common phenomenon with respect to solar power in subtropical regions, where sunny, arid regions are found on the western side of continents as a result of atmospheric circulation cells.

The model uses the diurnal curves in Figure 5 to calculate a dyad's annual average revenue and to determine the potential solar contribution for every hour, taking into account restrictions imposed by the assumed turndown rate. This is an obvious simplification, as it incorporates average *annual* diurnal variation but ignores *seasonal* variation altogether. It also assumes that power consumption throughout the day follows a similar pattern for all locales, but tropical areas will likely have "flatter" load curves than those exhibited by more temperate climates for which data was available. Collection of load and price data for a greater number of locales would allow for better specification of diurnal and seasonal trends.

Baseline average revenue per kWh varies by country. The simplified approach used here assumes that the price of electricity (heavily subsidized in some countries) is a political decision and taken as given and unchanging (in real terms) over time. This is a conservative assumption and will tend to overestimate the cost of GHG abatement, since the global trend is towards higher, not lower, electricity prices as result of both increasing fossil fuel prices and pressure to eliminate subsidies. Reported retail electricity prices were collected for about 75 countries worldwide, U.S. states, and 15 European cities (E-Control and VaasaETT 2009; EIA 2010; World Bank 2010). When needed, the retail price is reduced ~20% to reflect the typical share attributable to distribution in the U.S. Value-added taxes are also subtracted out for European countries (EC 2010). The resulting value is the average revenue per kWh to the generator (Figure 6).[9] Countries without data are assigned a value of 6 cents per kWh, equal to the assumed values for China and India.

Figure 6: Assumed average electricity price for major economies, net of taxes and distribution

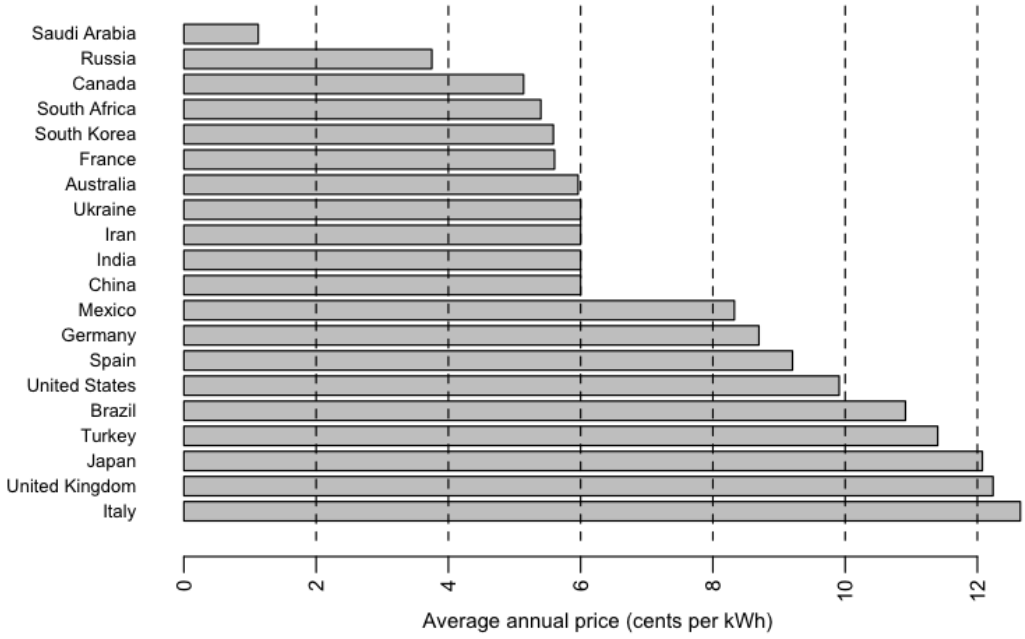

[9] An alternative approach is to estimate the "shadow price" – the expected price of electricity in the absence of market distortions (subsidies). In terms of calculating the additional cost of solar power, the shadow price may be more appropriate if it is possible to shift existing subsidies. Given that there is no global market for electricity and the cost of production can differ significantly between locales even for the same generating technology, estimating a shadow price is difficult. Consequently, the approach here uses the retail electricity price and simply notes that required solar power subsidies may be less than estimated on this basis.

Solar power averts emissions from counterfactual coal power plants. The total abatement is the difference in life-cycle emissions between the chosen solar technology and the reference coal technology. A value of ~900 gCO_2-eq per kWh is used as a global estimate for direct emissions from supercritical coal combustion (Wang and Nakata 2009). In addition to this direct mitigation is the indirect avoidance of GHG emissions associated with upstream (coal mining, transport, and plant construction) and downstream (decommissioning and waste disposal) processes over the lifetime of a plant. Estimates of the indirect component are less certain; 175 gCO_2-eq per kWh is taken as representative of existing studies (Weisser 2007). Life cycle emissions for CSP and CSPTS are assumed to be 30 and 40 gCO_2-eq per kWh, using the values in Piemonte et al. (2010) as a guide. The GHG footprint of photovoltaic power is higher (90 gCO_2-eq per kWh) due to the significant energy required to extract and process materials (Evans et al. 2009).

VI. GLOBAL SIMULATION OF DEPLOYMENT

A simulation is run with a deployment target of 2,000 TWh of utility-scale solar power in 2030. This target is commensurate with the additional contribution from CCS (1,600 TWh), wind power (2,600 TWh), and nuclear power (2,700 TWh) by 2030 in the IEA's 450 ppm CO_2-eq stabilization scenario. A contribution of 2,000 TWh per year is equivalent to ~10% of current consumption and ~6-7% of 2030 consumption, depending on energy efficiency assumptions.

There are no restrictions on the geographic sourcing of solar power; the model is free to transmit electricity via any dyad, regardless of geopolitical considerations, as long as the cost of coal power GHG abatement is minimized. The results are clearly removed from political reality, but it is important to understand where the idealized (optimal) deployment schemes face geopolitical obstacles. Figure 7 shows the production and consumption sites and connecting transmission corridors identified as optimal. Since the model does not (yet) incentivize consolidation of line routes, the results tend to proliferate spatially; in practice, the number of corridors would be lower. The range of corridor capacities is restricted at the upper end to improve visualization. A small but critical number of connections – like the trunk lines running west-to-east across North America and China, north-to-south from North Africa to Europe, and from the Persian Gulf to India are actually rated upwards of 50 GW, with high-traffic segments reaching over 100 GW. These capacities far exceed anything currently in operation. For comparison, the transmission infrastructure dedicated to China's Three Gorges Dam has a total capacity of ~19 GW.

Figure 7: Primary utility-scale solar power transmission corridors in 2030

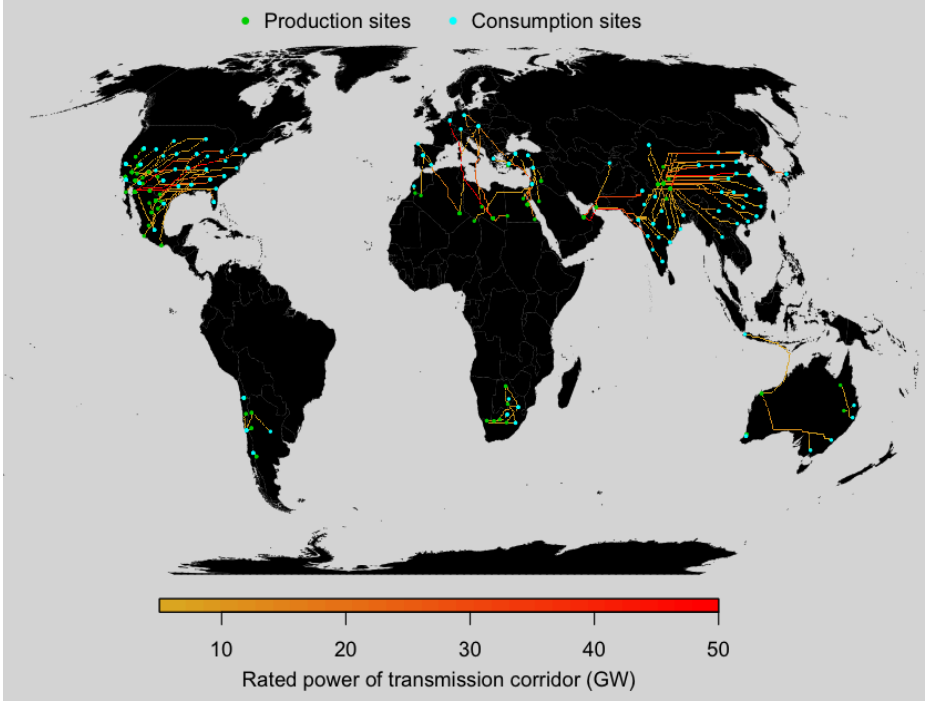

As described in Section V, consumption and production are determined for unique zones. In order to give an idea of the approximate spatial distribution of solar power consumption in 2030, each zone's total is disaggregated across space using patterns in future consumption to allocate (Figure 8). Figure 9 reports country totals.

Figure 8: Approximate distribution of utility-scale solar power consumption in 2030

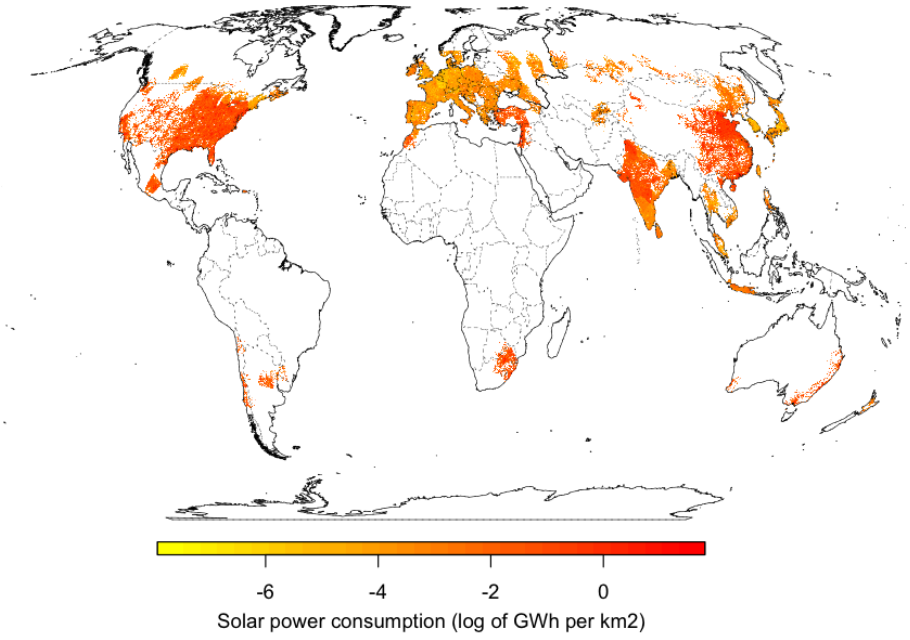

Figure 9: Top utility-scale solar power consumers in 2030

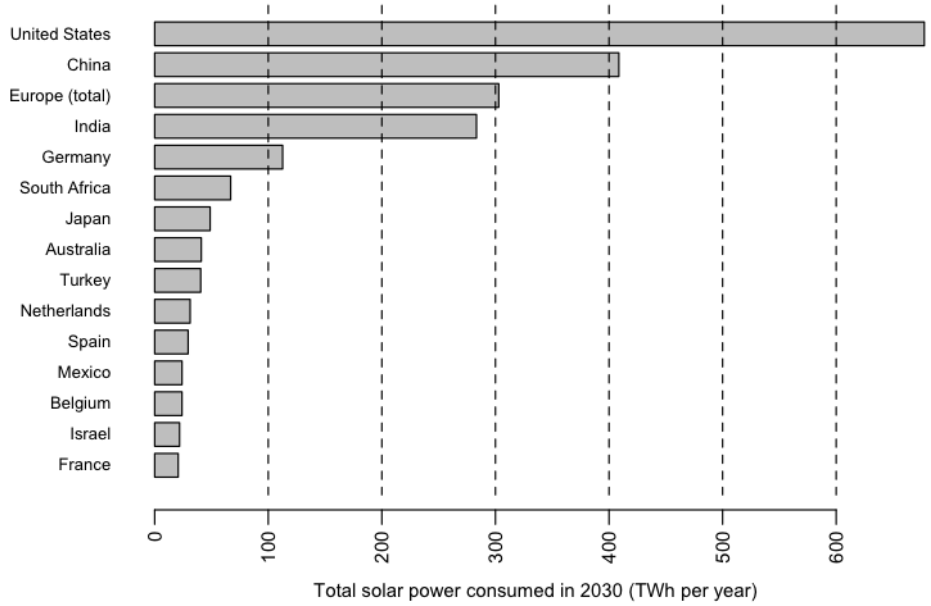

The geographic distribution of new solar builds changes significantly over time. Figure 10 shows the breakdown of new solar power consumption by period and region. Deployment begins in North America, utilizing short-distance transmission within the U.S. and long-distance transmission from low-cost locales in northern Mexico. The U.S. remains the dominant consumer over the next decade. Beginning in the 2020's, consumption diversifies as Europe and India import large quantities of solar power and Australia develops its domestic resources. By the end of the 2020's, China and India dominate the utility-scale solar market, accounting for more than 75% of new consumption in the latter half of the decade. A significant amount of solar power is consumed in the Near East, primarily Turkey and Israel (included in "Other" category; Figure 10), with power sourced from prime sites in Turkey, Iraq, and Egypt.

Figure 10: New utility-scale solar power consumption by period and region

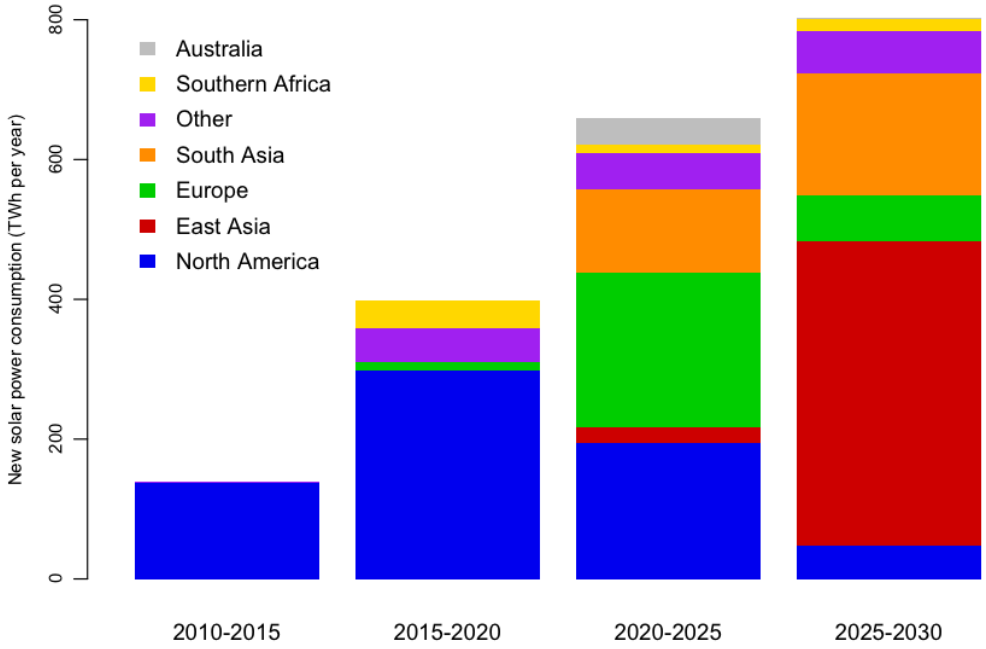

The combined effect of coal plant retirements, consumption trends, electricity prices, and geographic circumstances determine the extent to which a country can utilize solar power. Model output suggests a number of major consumers could rely upon utility-scale solar for a significant share of future electricity consumption (Figure 11). These numbers are by no way predictive, since the model does not account for trade-offs against other renewable power technologies that may be preferable. Figure 11 does suggest, however, the *potential* for considerable solar power penetration in Germany, South Africa, Australia, the U.S., and India.

Figure 11:Utility-scale solar power consumption in major economies in 2030

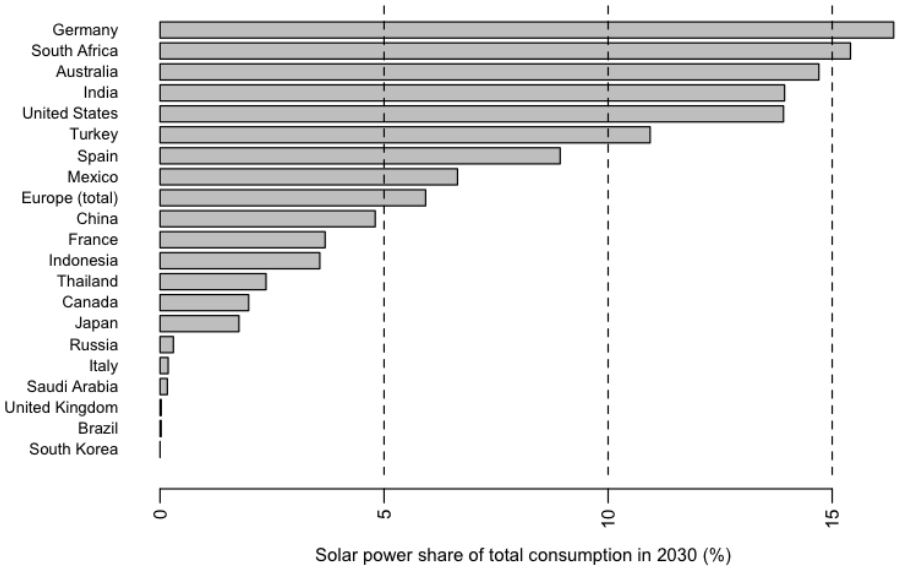

Because the simulation allows for maximum cross-border transmission of electricity – *even in cases where it may be practically impossible for geopolitical reasons* – there is significant importing and exporting (Figure 12). Only about 30% of consumption in the simulation is met by domestic supply. This would be the case in nearly any political scenario for Europe, which has very little low-cost, utility-scale solar potential of its own and must rely upon North Africa (primarily Libya and Egypt). For India, which *does* have resources of its own, the model still suggests that optimal GHG abatement occurs by importing large amounts of power from both China and the Persian Gulf. This is because the quality of solar resources in those locales is sufficiently higher than those in India to offset the additional cost of transmission. The model also relies upon Mexican generating sites to provide about 80% of U.S. solar power consumption, though this arrangement offers minimal advantage over sites in the U.S. southwest. Testing alternative model specifications can reveal the extent to which restricting cross-border transmission increases the cost of abatement (see below).

Figure 12: Major importers and exporters of solar power in 2030

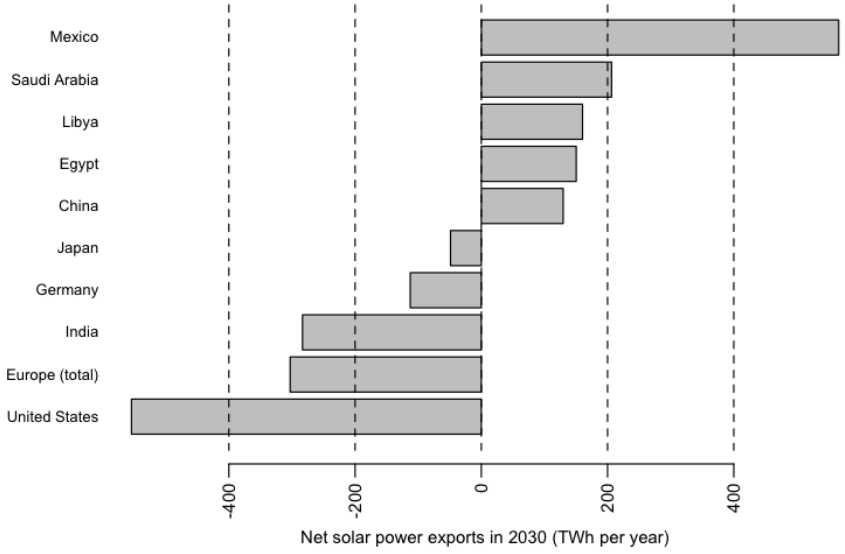

The solar power expansion provides total abatement of ~63 $GtCO_2$-eq over the lifetime of facilities in operation by 2030. The cost of achieving that abatement depends on the assumed discount and learning rate. The latter describes how quickly the cost of production falls in response to deployment as a result of returns to scale, mass manufacturing, improved technology, etc. Experience with solar and other alternative energy technologies shows that capital costs typically fall 5% to 20% for every doubling of installed capacity (Junginger et al. 2008; Neij 2008). Different technologies exhibit different learning rates. For example, cost reductions for photovoltaics have tended to be faster given their modular design and scalability in manufacturing. For this analysis, however, the learning rate is assumed to be constant across technologies.[10]

[10] Interestingly, the model almost universally prefers CSP without storage to either PV or CSPTS. The only way to really explore the robustness of this finding is to test many models runs with varied cost assumptions (both for the generating technologies and transmission). The question of technology preference is further complicated by the fact

If the levelized cost of production, including transmission, is greater than the expected average revenue, a subsidy is needed to cover the difference. Since the subsidy payments could be made over the 30-year lifetime of a plant (as in a perpetual feed-in tariff), the present value of the subsidy is only a fraction of the nominal total. The overall cost of abatement is *highly* sensitive to the assumed learning and discount rate. This is evidenced in Figure 13, which gives the average (program-wide) abatement cost surface for a range of assumptions. Assuming learning and discount rates equal to 5%, the average cost of abatement is ~$35 per tCO_2-eq. Increasing the learning and discount rates by just 2 percentage points (to 7%), reduces the cost of abatement to nearly $20 per tCO_2-eq.

Figure 13: Average cost of abatement, alternative discount and learning rates

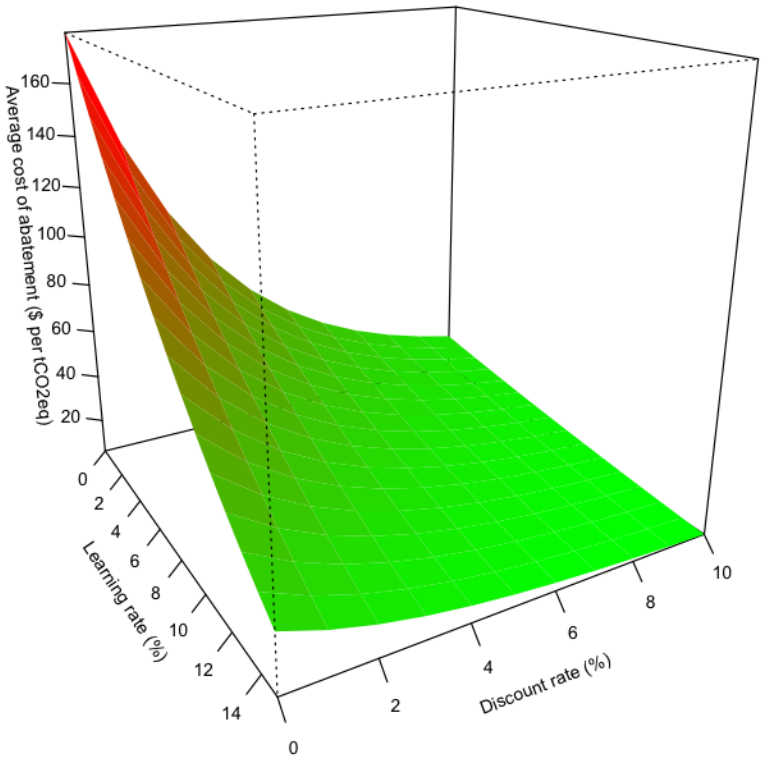

Figure 14 shows the trend in the abatement cost for new solar builds over time, assuming a discount rate of 5%. The top curve shows the average (lifetime) abatement cost of new builds if there are no learning effects. The line slopes upward, reflecting the consequences of moving to more costly locales. The middle curve shows the effect of the learning rate; cost reductions due to learning are nearly able to offset the consequences of tapping increasingly costly sites. The middle curve also gives the approximate price required in future carbon markets for solar projects to be viable. The lower curve consists of all costs discounted back to the present.

---

that PV may be capable of faster cost reductions than CSP. In that case, learning rate effects would need to be modeled internally rather than after-the-fact as presently done.

Figure 14: Marginal cost of GHG abatement for future solar power builds

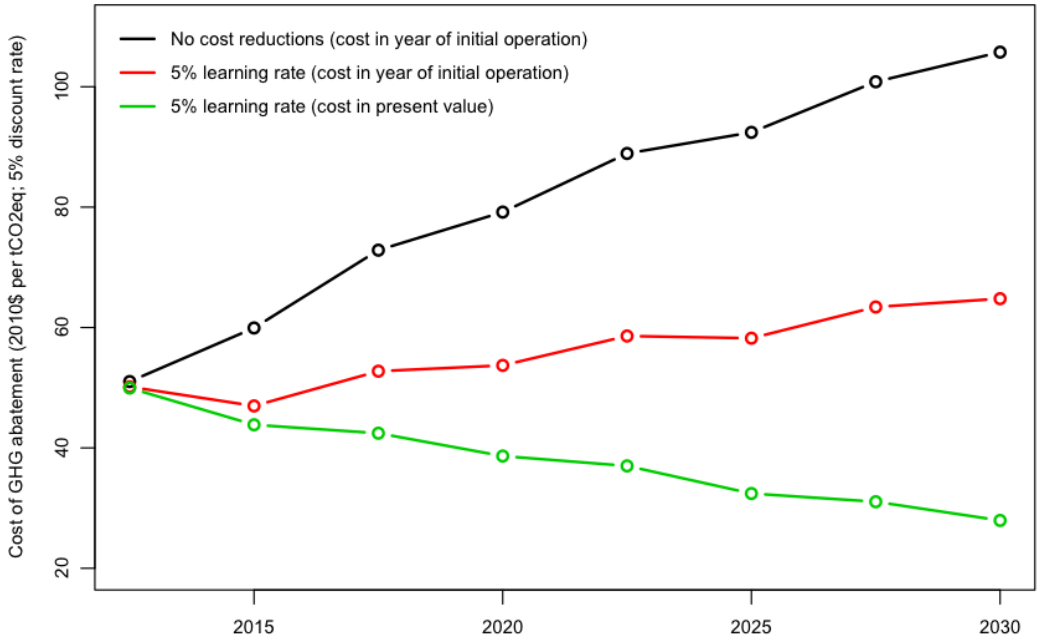

An alternative scenario was modeled in which *no* cross-border transmission is allowed – all solar power must come from within country. This restriction only increases the overall cost of abatement by ~10%, though it does alter the patterns of distribution. In particular, solar power consumption is eliminated in Europe and reduced by ~40% in India, offset by increased consumption in China. The U.S. eliminates solar power imports from Mexico by shifting to domestic production sites in the southwest. This scenario is substantially different in terms of geopolitics and transmission, but the cost structure is only marginally impacted.

VII. Discussion

High-resolution assessment of utility-scale solar power potential shows that a number of countries have extensive resources at their disposal. The lowest-cost locales include northern Mexico and the American southwest, parts of the South American Andes and Patagonia, the Sahel and Middle East, southern Africa, the Tibetan Plateau, and Australia. These areas offer opportunities for low-cost production but are often far from consumption centers. Long-distance transmission can be a cost-effective tool for GHG abatement if sufficiently large amounts of power are transmitted to locales with relatively high electricity prices, especially if consumption is located east of production in order to take advantage of diurnal variations in prices and load.

A global simulation designed to provide 2,000 TWh of utility-scale solar power by 2030 results in a distinctive pattern of deployment over time and space. If the goal is to maximize climate change mitigation for each dollar of solar power subsidy worldwide, the results suggest financial incentives would be focused in North America over the next decade, diversifying to Europe and India by the early 2020's, and concentrating in China in the second-half of the decade. If cross-border transmission is curtailed or eliminated, the pattern of deployment shifts even more toward China, with significant

production occurring by the early 2020's. Given the level of solar power deployment modeled here, these findings suggest that nearly-optimal *global* GHG abatement could be achieved while still allowing 10-15 years in which to secure the political support, financing, and transmission planning necessary for large-scale penetration in Chinese markets by the mid-2020's. It must be stressed, however, that the optimal amount of *overall* solar penetration remains an open question, since this analysis does not assess alternative generating technologies also capable of reducing emissions.[11]

Overall, transmission requirements increase production costs by ~18%. The primary long-distance transmission routes are those running from the American southwest to the midwest and northeast, from Egypt and Libya to central Europe via Mediterranean crossings, from Saudi Arabia to northwest India via a Persian Gulf crossing, and from the Tibetan Plateau to both India and major cities in East Asia. Less prominent flows include those within the Near East (from Egypt and Iraq to Turkey and Israel, primarily); southern Africa (meeting demand in South Africa with domestic sites and imports from Namibia and Botswana); and Australia. A potential linkage is identified between high-quality sites near the Western Australia coast and Indonesia, via a submarine cable. Line routing accounts for barriers and additional cost imposed by rough terrain, though running the model at higher spatial resolution would provide more concrete results (for example, whether sufficient corridors can be identified through the Himalayas).

The cost of expansion depends heavily on the assumed rate of technology learning and discounting. At moderate levels (5%) for both, the average cost of GHG abatement in present terms is ~$35 per tCO_2-eq. At 7% learning and discount rates, the average cost falls to ~$20 per tCO_2-eq. The marginal cost of abatement for new builds (assuming 5% learning rate) increases only slightly over time, rising from ~$50 per tCO_2-eq at present to ~$65 per tCO_2-eq in 2030. Interestingly, modeling of global carbon markets in a 450 ppm CO_2-eq stabilizaton scenario suggests the price by 2030 could be ~$65-70 per tCO_2-eq (IEA 2009). This suggests that even at relatively low learning and discount rates, utility-scale solar power would be a viable investment for climate mitigation at deployment levels of at least 2,000 TWh per year by 2030. Preliminary evidence suggests that eliminating cross-border transmission of electricity only marginally increases the overall cost of abatement (~10% increase), implying that near-optimal GHG abatement via utility-scale solar power does not *necessarily* depend upon large-scale electricity importing that might be politically untenable.

These findings are illustrative rather than predictive. Carbon taxes in Europe, for example, may spur the import of North African solar power sooner than suggested here. But the differences between what is *likely* to occur and what is *optimal* in terms of GHG abatement are important to consider, especially for donors and governments interested in strategic planning for long-term mitigation of climate change. Such planning often includes tough choices about how to disperse industry subsidies that, once captured, are difficult to redirect. Further, the lead-time for arranging financing and transmission infrastructure can be significant, requiring a clear idea of where and when investments are likely to have the most impact. The

[11] The overall level of desired abatement will also affect the pattern of deployment across regions and time. Though not explicitly tested here, it is probably safe to assume that larger solar deployment targets would require faster (i.e. sooner) introduction to Indian and Chinese markets. How early these technologies must be deployed in the developing world is, in part, dictated by the rate of coal plant retirements in developed countries – if there is sufficient coal to displace, deployment can be focused in developed countries longer while still minimizing the cost of abatement. At some point, however, massive growth in consumption coupled with retirement of 1990's-era coal plants in India and China will necessitate a shift if abatement costs are to remain low.

cost of GHG abatement is not the only consideration when promoting renewable energy, but it is an important one – and one that is not immediately obvious using conventional modes of analysis.

There is much room for improvement in the area of spatially-explicit energy modeling. In particular, better data inputs and high-resolution modeling runs could provide more accurate results. Ultimately, the value of such models lies in their potential application to a wide array of research questions. Bringing larger computing resources to bear could allow multiple scenarios to be quickly compared, helping inform decision-making in the following areas:

Geopolitics and energy security

Models can be configured to test the impact of geopolitical concerns on overall solar power cost and abatement potential. Scenarios allowing import and export among various groupings of countries can help determine the cost (in increased solar subsidies or forgone export revenue) of restricting transmission flows to and from allies or forcing transmission lines to traverse "friendly" terrain. Large-scale renewable power also entails the risk of terrorist attacks on critical transmission lines. The cost of any single attack is lowered by reducing reliance on major corridors and spreading transmission across spatially-diffuse lines. A transmission algorithm could be modified to, for example, allow a maximum percentage of a country's supply to be routed through any single corridor. Such model runs could help identify the additional cost of addressing legitimate fears over physical energy security.

Environmental protection and land use

Land use and siting of large renewable energy projects is a major issue, especially in countries with strong environmental regulations. A spatially-explicit model can help reveal the additional cost of moving projects away from, for example, ecologically sensitive regions. It can also test the additional cost of *not* allowing construction in protected areas, or the effect of allowing development on grasslands or rainfed cropland (excluded in the analysis presented here), which may be significantly closer to consumption centers. This knowledge is useful in terms of setting national land-use policies and granting permits for projects.

Water usage

The consumption of water resources for power generation is potentially troublesome in the case of CSP technologies, which need to be located in places with little cloud cover and precipitation and can use as much water as conventional thermal generation if evaporative cooling is employed. A water use module could calculate the total water requirements alongside cost and GHG abatement a well as test the additional cost of forcing CSP to utilize "dry-cooling" technology, which can reduce water consumption by ~95% but imposes an efficiency penalty (DOE 2010). Since water availability is inherently spatial, it is possible to configure a model to deploy plants only in locales where water resources are close by or available via rainwater catchment and storage.

Transmission planning and technology

Even at relatively modest resolution, model runs can identify the likely path of major transmission corridors. This is potentially important information in facilitating national (or even multinational) planning, especially since the lead-time for such projects could be significant. The cost and technical characteristics of transmission technology are important parameters in scenarios exploring cross-border and long-distance transmission. It is possible to test the consequences of technological breakthroughs in transmission technology – for example, higher line voltages or introduction of superconductors – on the overall cost of greenhouse gas abatement.

Optimization of renewable energy supports

Perhaps most importantly, spatially-explicit models can help inform renewable energy policy by identifying the technological choices, location, and timing of optimal deployment and required subsidies. This will require integration of multiple technologies, including non-renewables like nuclear power and CCS that have spatial attributes that are rarely accounted for. Domestic and international actors disperse energy subsidies for many reasons – often political and unrelated to climate mitigation – but identifying the strategies most conducive to reducing emissions would provide important guidance that is missing at present.

REFERENCES

Aboumahboub, T., Tzscheutschler, P., and Hamacher, T. 2010. Optimizing world-wide utilization of renewable energy sources in the power sector. Presented at the International Conference on Renewable Energies and Power Quality, 23-25 March, Granada, Spain.

Bicheron, P., Defourny, P., Brockmann, C., Schouten, L., Vancutsem, C., Huc, M., Bontemps, S., Leroy, M., Achard, F., Herold, M., Ranera, F., and Arino, O. 2008. Globcover: products description and validation report. ESA Globcover Project led by MEDIAS France/POSTEL.

Czisch, G. 2006. Realisable scenarios for a future electricity supply based 100% on renewable energies. Unpublished manuscript. Available at: http://130.226.56.153/rispubl/reports/ris-r-1608_186-195.pdf

CIGRE. 2009. Impacts of HVDC lines on the economics of HVDC projects. International Council on Large Electric Systems, Joint Working Group B2/B4/C1.17.

Denholm, P. and Margolis, R. 2006. Very large-scale deployment of grid-connected solar photovoltaics in the United States: challenges and opportunities. Presented at the Solar 2006 Conference, 8-13 July, Denver, Colorado.

Dijkstra, E.W. 1959. A note on two problems in connexion with graphs. *Numerische Mathematik* 1: 269-271.

DOE. 2008. 20% wind energy by 2030: increasing wind energy's contribution to U.S. electricity supply. U.S. Department of Energy, DOE/GO-102008-2567, July.

DOE. 2010. Reducing water consumption of concentrating solar power electricity generation. U.S. Department of Energy. Report to Congress. Available at: http://www.nrel.gov/csp/pdfs/csp_water_study.pdf

EC. 2010. Excise duty tables: energy products and electricity. European Commission. Available at: http://ec.europa.eu/taxation_customs/resources/documents/taxation/excise_duties/energy_products/rates/excise_duties-part_II_energy_products-en.pdf

E-Control and VaasaET. 2009. European household electricity price index for Europe (HEPI). Available at: http://www.vaasaett.com/wp-content/uploads/2009/08/HEPI-Press-Release-June.pdf

EIA. 2010. Monthly electric sales and revenue report with state distributions report. U.S. Energy Information Administration, Form EIA-826. Available at: http://www.eia.doe.gov/cneaf/electricity/epm/table5_6_b.html

EnerNex. 2010. Eastern wind integration and transmission study. Prepared for the National Renewable Energy Laboratory. Subcontract report NREL/SR-550-47078.

EPRI. 2006. EPRI-GTC overhead electric transmission line siting methodology. Electric Power Research Institute and Georgia Transmission Corporation.

Evans, A., Strezov, V., and Evans, T.J. 2009. Assessment of sustainability indicators for renewable energy technologies. *Renewable and sustainable energy reviews* 13: 1082-1088.

FAO, IIASA, ISRIC, ISSCAS, and JRC. 2009. Harmonized world soil database (version 1.1). Food and Agriculture Organization, Rome, Italy and International Institute for Applied Systems Analysis, Laxenburg, Austria.

GE Energy. 2010. Western wind and solar integration study. Prepared for the National Renewable Energy Laboratory. Subcontract report NREL/SR-550-47434.

Gilman, P., Blair, N., Mehos, M., Christensen, C., Janzou, S., and Cameron, C. 2008. Solar advisor model user guide for version 2.0. National Renewable Energy Laboratory Report No. TP-670-43704.

Hijmans, R.J., Cameron, S.E., Parra, J.L., Jones, P.G., and Jarvis, A. 2005. Very high resolution interpolated climate surfaces for global land areas. *International Journal of Climatology* 25: 1965-1978.

Hijmans, R.J. and Van Etten, J. 2010. Raster: geographic analysis and modeling with raster data. R package version 1.3-11. Available at: http://R-Forge.R-project.org/projects/raster/

IEA. 2009. World energy outlook 2009. International Energy Agency, Paris.

(IPCC) Barker, T., Bashmakov, I., Alharthi, A., Amann, M., Cifuentes, L., Drexhage, J., Duan, M., Edenhofer, O., Flannery, B., Grubb, M., Hoogwijk, M., Ibitoye, F.I., Jepma, C.J., Pizer, W.A., Yamaji, K. 2007. Mitigation from a cross-sectoral perspective. In *Climate Change 2007: Mitigation*. Contribution of Working Group III to the Fourth Assessment Report of the Intergovernmental Panel on Climate Change [B. Metz, O.R. Davidson, P.R. Bosch, R. Dave, L.A. Meyer (eds)], Cambridge University Press, Cambridge, United Kingdom and New York, NY, USA.

IUCN and UNEP. 2010. World database on protected areas (WDPA). International Union for Conservation of Nature and United Nations Environment Programme (World Conservation Monitoring Centre), Cambridge, United Kingdom.

Junginger, M., Lako, P., Lensink, S., van Sark, W., and Weiss, M. 2008. Technological learning in the energy sector. Netherlands Research Programme on Scientific Assessment and Policy Analysis for Climate Change, April.

Li, Y. and Flynn, P.C. 2004. Deregulated power prices: comparison of diurnal patterns. *Energy Policy* 32: 657-672.

NASA. 2009. Surface meteorology and solar energy (version 6.0). Obtained from the NASA Langley Research Center Atmospheric Science Data Center.

Neij, L. 2008. Cost development of future technologies for power generation – a study based on experience curves and complementary bottom-up assessments. *Energy Policy* 36 (6): 2200-2211.

NOAA. 2009. DMSP-OLS nighttime lights time series (1992-2008). Image and data processed by the National Oceanic and Atmospheric Administration's National Geophysical Data Center; DMSP data collected by U.S. Air Force Weather Agency. Available at: http://www.ngdc.noaa.gov/dmsp/downloadV4composites.html

NREL. 2005. Monthly and annual average direct normal irradiance at 40km resolution. National Renewable Energy Laboratory, Golden, Colorado. Available from the Solar and Wind Energy Resource Assessment (SWERA/UNEP). Available at: http://swera.unep.net/

ORNL. 2008. LandScan™ global population dataset. Oak Ridge National Laboratory, Oak Ridge, Tennessee.

Piemonte, V., De Falco, M., Tarquini, P., and Giaconia, A. 2010. Life cycle assessment of a high temperature molten salt concentrated solar power plant. Presented at 20th European Symposium on Computer Aided Process Engineering.

Sullivan, P., Logan, J., Bird, L., and Short, W. 2009. Comparative analysis of three proposed federal renewable electricity standards. NREL Technical Report TP-6A2-45877.

Ummel, K. 2010. Concentrating solar power in China and India: a spatial analysis of technical potential and the cost of deployment. Working Paper No. 219, Center for Global Development, Washington, D.C.

Ummel, K. and Wheeler, D. 2008. Desert power: the economics of solar thermal electricity for Europe, North Africa, and the Middle East. Working Paper No. 156, Center for Global Development, Washington, D.C.

Verdin, K.L., Godt, J.W., Funk, C., Pedreros, D., Worstell, B., and Verdin, J. 2007. Development of a global slope dataset for estimation of landslide occurrence resulting from earthquakes. United States Geologic Survey, Colorado, Open-File Report 2007-1188.

Van Eeckhout, B., Van Hertem, D., Reza, M., Srivastava, K., and Belmans, R. 2010. Economic comparison of VSC HVDC and HVAC as transmission system for a 300 MW offshore wind farm. *European Transactions on Electrical Power* 20: 661-671.

Van Etten, J. 2010. Gdistance: distances and movements on geographical grids. R package version 1.0. Available at: http://R-Forge.R-project.org/projects/gdistance/

Wang, H. and Nakata, T. 2009. Analysis of the market penetration of clean coal technologies and its impacts in China's electricity sector. *Energy Policy* 37 (1): 338-352.

Weisser, D. 2007. A guide to life-cycle greenhouse gas (GHG) emissions from electric supply technologies. *Energy* 32 (9): 1543-1559.

Wheeler, D. 2010. Fair shares: crediting poor countries for carbon mitigation. Center for Global Development Working Paper (forthcoming), Washington, D.C.

Wheeler, D. and Shome, S. 2010. Less smoke, more mirrors: where India really stands on solar power and other renewables. Working Paper No. 204, Center for Global Development, Washington, D.C.

Wheeler, D. and Ummel, K. 2008. Calculating CARMA: global estimation of CO_2 emissions from the power sector. Working Paper No. 145, Center for Global Development, Washington, D.C.

World Bank. 2010. Africa infrastructure country diagnostic database. Available at: http://ddp-ext.worldbank.org/ext/DDPQQ/member.do?method=getMembers&userid=1&queryId=278

Zhang, Y., Smith, S.J., Kyle, G.P., Stackhouse, P.W. 2010. Modeling the potential for thermal concentrating solar power technologies. *Energy Policy* 38 (12): 7884-7897.